



# Insight into the strong inhibitory action of salt on activity of neocarzinostatin

Der-Hang Chin \*, Huang-Hsien Li, Christopher G. Sudhahar, Pei-Yin Tsai

Department of Chemistry, National Chung Hsing University, 250 Kuo-Kuang Road, Taichung, Taiwan 40227, ROC

## ARTICLE INFO

### Article history:

Received 18 November 2009

Revised 12 January 2010

Accepted 13 January 2010

Available online 18 January 2010

### Keywords:

Drug activity

DNA cleavage

Neocarzinostatin

Enediyne antibiotics

Antitumor

## ABSTRACT

Enediyne anticancer drugs belong to one of the most potent category in inducing DNA damage. We report  $85 \pm 5\%$  inhibition on activity of neocarzinostatin by salt. As high sodium ion concentration is a known tumor cell feature, we explored the dynamic mechanism of inhibition. Using various analytical tools, we examined parameters involved in the four consecutive steps of the drug action, namely, drug releasing from carrier protein, drug–DNA binding, drug activating, and DNA damaging. Neither protein stability, nor drug release rate, was altered by salt. The salt inhibition level was similar in between the protein-bound and unbound enediyne chromophore. Salt did not quench the thiol-induced drug activation. The inhibition was independent of DNA lesion types and irrelevant with thiol structures. Collectively, no salt interaction was found in the releasing, activating, and DNA damaging step of the drug action. However, binding with DNA decreased linearly with salt and corresponded well with the salt-induced inhibition on the drug activity. Salt interference on the affinity of DNA binding was the main and sole cause of the severe salt inhibition. The inhibition factor should be carefully considered for all agents with similar DNA binding mode.

© 2010 Elsevier Ltd. All rights reserved.

## 1. Introduction

The enediyne antibiotic category is among the most effective antitumor agents and has been the focus of intensive research because of its extremely potent activity and intricate mode of action. Neocarzinostatin (NCS)<sup>1,2</sup> is the first naturally occurring enediyne member. We reported earlier that variation of a thiol activator may cause threefold reduction in the NCS activity.<sup>3</sup> In the present study we focused on the effect of ordinary salt, which resulted in nearly sevenfold reduction ( $85 \pm 5\%$  inhibition) in the NCS-mediated DNA lesions. As high intracellular  $\text{Na}^+$  content is a common tumor cell feature,<sup>4</sup> exploring the salt inhibition mechanism can provide significant implications in cancer chemotherapy.

The NCS chromoprotein (holoNCS) is a 1:1 non-covalent complex of a labile chromophore (NCS-C) (MW = 659) and a tightly bound protein (apoNCS) (113 amino acids).<sup>5</sup> The antitumor activity solely arises from the DNA damaging agent NCS-C, whose chemical structure involves an active enediyne ring<sup>2</sup> along with a naphthoate and an amino sugar moiety<sup>6</sup> (see Scheme 1a for NCS-C

structure). The apoNCS shows no DNA damaging activity, but stabilizes NCS-C and serves as a carrier to deliver the labile NCS-C to the target DNA.<sup>7</sup>

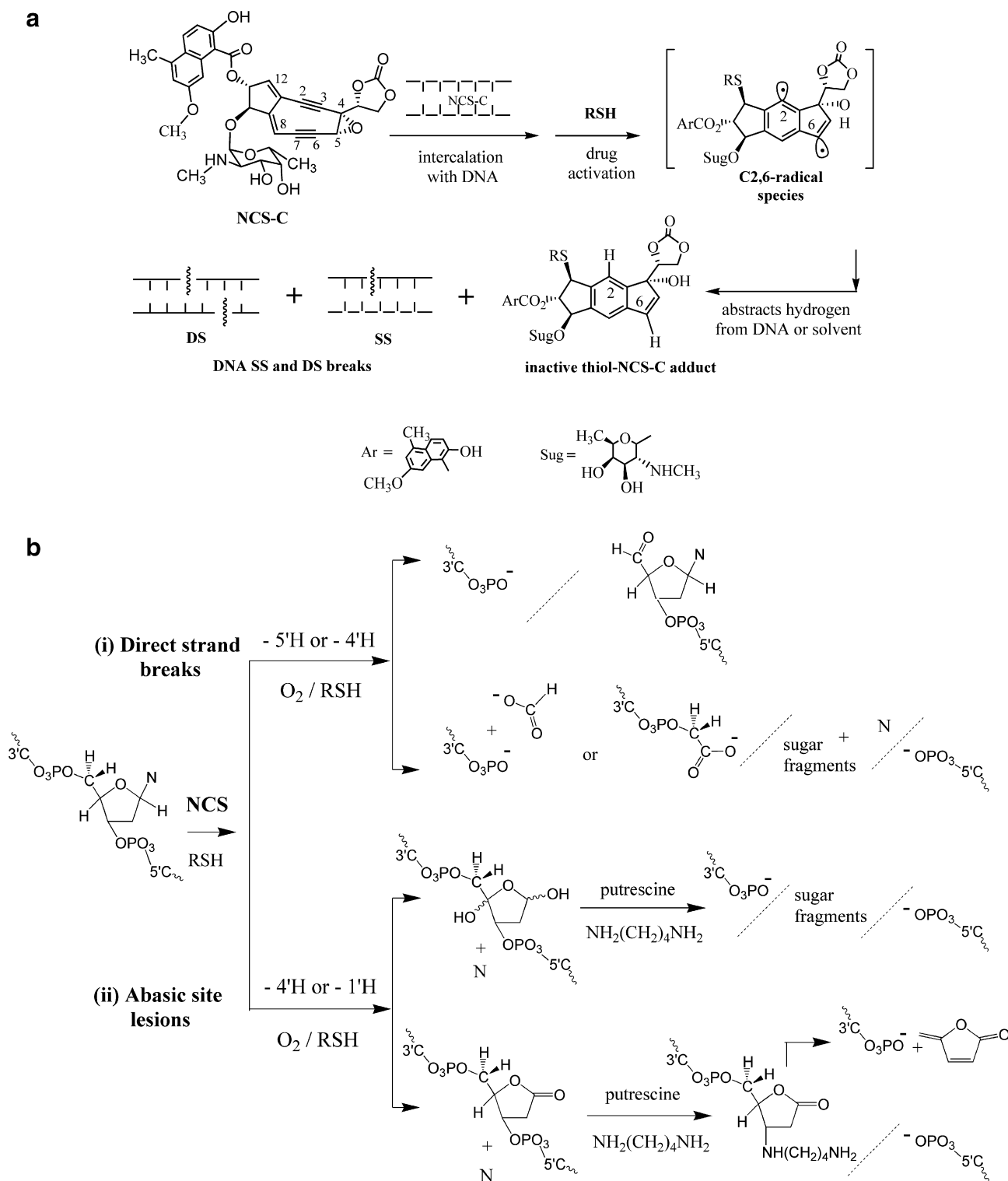
As no interaction was found between apoNCS and DNA in the NCS-mediated DNA lesion reactions,<sup>8</sup> controlled release of NCS-C from holoNCS has to be the first step in the mode of NCS action. Early kinetic data suggested that NCS-C binds to DNA prior to undergoing thiol-induced activation of the drug.<sup>9</sup> The binding involves intercalating the naphthoate moiety of NCS-C in between base pairs of the DNA double strand, which affords protection of NCS-C from spontaneous degradation.<sup>10,11</sup> Following DNA binding, a thiolate attack on C-12 of NCS-C cascades an irreversible activation reaction (Scheme 1a). The enediyne moiety is transformed into a transient C2,6-radical intermediate,<sup>12</sup> which abstracts hydrogen atoms from DNA or solvent<sup>13</sup> to form a stable and inactive thiol–NCS-C adduct. Because of binding preference, the hydrogen abstraction mainly occurs at DNA sugar moiety of T and A residues.<sup>5</sup> Molecular oxygen and thiol are involved in the subsequent oxidative reactions, which lead to single-strand (SS) and double-strand (DS) DNA lesions. The DS type of lesion, though in a much less extent, is more lethal than SS one and is considered to correlate with the level of cell killing in human tumors.<sup>14</sup>

The NCS-induced DNA lesion is chemically expressed into two forms: direct strand breaks and abasic site lesions (Scheme 1b). About 80% of the direct strand breaks occurs at 5'-position of T residues to produce a 5'-aldehyde end.<sup>15,16</sup> To a lesser degree, generation of formate<sup>17</sup> (by 5'-H abstraction) or 3'-phosphoglycolate<sup>18</sup> (by 4'-H abstraction) also results in direct strand breaks

**Abbreviations:** NCS, neocarzinostatin; NCS-C, neocarzinostatin chromophore; apoNCS, apoprotein component of neocarzinostatin; holoNCS, chromoprotein complex of neocarzinostatin; CD, circular dichroism;  $T_m$ , temperature at which half of the protein is unfolded; HPLC, high performance liquid chromatography; BME, 2-mercaptoethanol; GSH, glutathione; Tris, tris(hydroxymethyl)-aminomethane; P:D, molar ratio of DNA nucleotide phosphorus to drug; SS, single-strand (breaks or lesions of DNA); DS, double-strand (breaks or lesions of DNA); TS, total strand (breaks or lesions of DNA); ct-DNA, calf-thymus DNA.

\* Corresponding author. Tel.: +886 4 22840411x304; fax: +886 4 22862547.

E-mail address: [chdhchin@dragon.nchu.edu.tw](mailto:chdhchin@dragon.nchu.edu.tw) (D.-H. Chin).



(Scheme 1b). The NCS-induced abasic site lesions (mainly by 4'-H or 1'-H abstraction), although minor in occurrence, shall not be ignored because they contribute very significant portion (about 83% in average)<sup>9</sup> in the lethal DS lesions. Abasic site lesions can be converted to strand breaks by alkaline treatment such as putrescine, which cleaves virtually all abasic sites.<sup>19</sup> While significant effect

on DNA-cleaving activity by the common cellular substance salt was observed, whether salt involves in any of these DNA damaging chemistries becomes an interesting question. Although NCS is very potent in inducing DNA damages, detailed understanding of factors that influence its biological activity is essential for the rational drug design.

## 2. Results

### 2.1. Analyses of salt effect on the NCS-mediated DNA lesion

The salt effect on the NCS activity was examined by analyzing the induced DNA direct strand breaks and putrescine-expressed total lesions. Putrescine was added after the NCS–DNA reaction to transform all abasic site lesions into strand breaks (Scheme 1b).<sup>3</sup> The DNA fragments were resolved in agarose gel electrophoresis and the number of strand breaks were analyzed by following the Poisson distribution in the conversion of supercoiled DNA (form I) into relaxed circular (form II) and linear duplex (form III) forms. Direct TS breaks and putrescine-expressed TS lesions in 0–700 mM NaCl were further quantified into SS and DS lesions.

#### 2.1.1. HoloNCS and NCS-C showed similar salt inhibition on activity

Figure 1a shows significant salt effect on the number of direct TS breaks mediated by BME-activated holoNCS or NCS-C. Low salt concentration at 25 mM already showed observable effect on the DNA damaging activity and the inhibition was more pronounced with increasing salt concentrations. The effect of salt was similar in both holoNCS- and NCS-C-mediated direct DNA cleavages. Figure 1b summarized the percentage of inhibition by salt on the putrescine-expressed DNA TS lesions induced by GSH-activated holoNCS or NCS-C. There were also no apparent differentials in TS lesions of holoNCS and NCS-C. The results confirmed the similarity in salt effect between the protein-bound and unbound NCS-C.

#### 2.1.2. Effect of salt on NCS activity was irrelevant with structure of thiol activators

The extent of DNA damage induced by NCS varies with thiol structures.<sup>3,9</sup> We employed different thiols to clarify whether thiol structure is involved in the salt inhibition mechanism. For comparison, the varied levels of DNA damage in the absence of salt were normalized to 100% or 0% inhibition. Figure 1b demonstrated similar % of salt inhibition in the BME- and GSH-activated holoNCS–DNA reactions. The results revealed that variation of thiol structure had insignificant influence on salt inhibition. Similar results were obtained when the extracted NCS-C was employed in place of holoNCS (data not shown), confirming minimum effect of thiol structure on salt inhibition mechanism.

#### 2.1.3. Salt inhibition level was alike in all types of DNA lesions

NCS-induced DNA direct strand breaks is predominant over abasic site lesions because of chemical preference (Scheme 1b), and SS lesions occur more frequently than DS ones.<sup>5</sup> Figure 1c shows the number of SS, DS, and TS breaks mediated by GSH-activated NCS-C after putrescine treatment. In the absence of salt, the number of SS, DS, and TS breaks/plasmid/ $\mu$ M NCS-C obtained were close to those reported.<sup>9</sup> With increasing salt concentrations, quantities of all types of DNA lesions gradually decreased following the similar trends.

#### 2.1.4. Overall salt inhibition on the NCS-mediated DNA lesion

The NCS-mediated DNA damage had similar trend of the salt inhibition in spite of NCS forms (holoNCS or NCS-C), thiol structures, or DNA lesion types (direct TS, SS or DS breaks or abasic site lesions). Table 1a shows the mean value averaged from the inhibition data obtained from reactions under various conditions. Inhibition increased sharply with increasing salt at a concentration below 300 mM. Beyond 300 mM, the salt-induced inhibition on the NCS activity gradually leveled off. At a concentration of 700 mM, the inhibition was up to  $85 \pm 5\%$ .

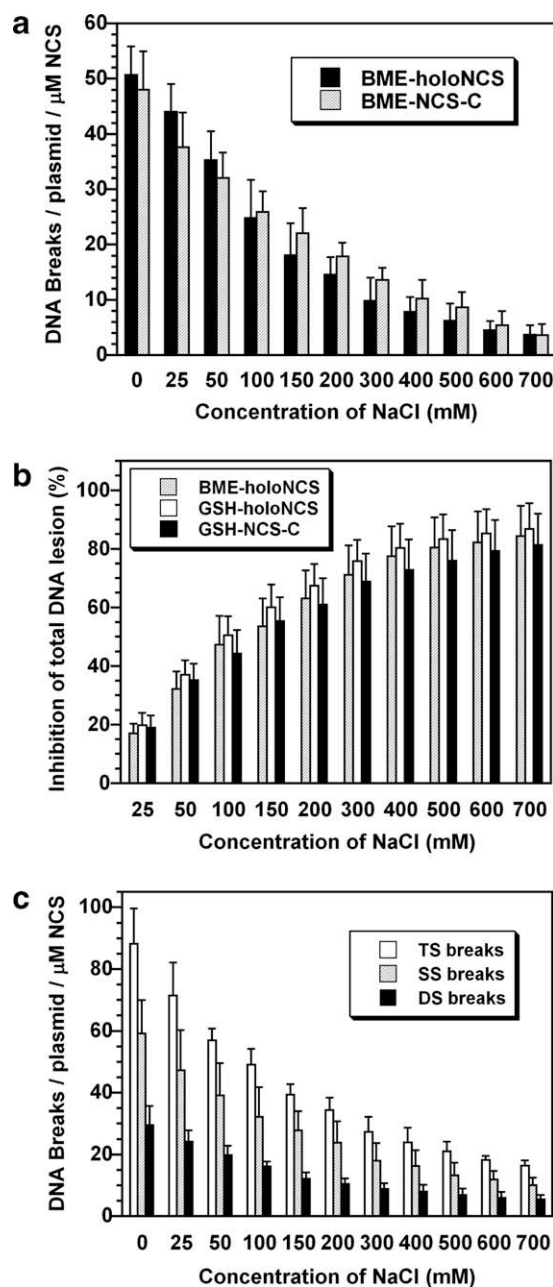


**Figure 1.** Effect of salt on NCS-mediated DNA lesions. (a) Direct strand breaks of DNA induced by BME-activated holoNCS (black bar) and NCS-C (hatched bar) in salt solutions. The drug–DNA reaction solutions were analyzed by electrophoresis without further putrescine treatment. (b) Salt-induced % of inhibition on total lesions of DNA resulted from BME-activated holoNCS (hatched bar), GSH-activated holoNCS (white bar), and GSH-activated NCS-C (black bar). The drug–DNA reactions were analyzed after putrescine treatment. (c) Total SS (hatched bar), DS (black bar), and TS (white bar) DNA lesions induced by GSH-activated NCS-C in salt solutions. The total lesions included direct strand breaks and abasic site lesions, which were converted to strand breaks after putrescine treatment. All values were averages of minimum 3 repeats and a cap on each bar represents standard deviation.

### 2.2. NCS protein was not involved in the salt inhibition mechanism

#### 2.2.1. Stability of NCS protein was unaltered by salt

Because conformational stability of NCS protein is crucial for protecting and regulating NCS-C,<sup>5,20</sup> we examined salt influence on the equilibrium unfolding properties of apoNCS. By monitoring changes of the far-UV CD signals at 224 nm,<sup>21</sup> conformational

changes of apoNCS were followed (Fig. 2a). In the absence of NaCl, the thermal unfolding of apoNCS at pH 7.0 showed a steep transition (about 0.061 mole fraction changes/°C) with a  $T_m$  (the temperature at which half of the protein is unfolded) at 64 °C. The results were consistent with early reports.<sup>21,22</sup> With salt, no significant changes on the protein stability could be observed at a salt concentration up to 1500 mM. As shown in Figure 2a, unfolding profiles and  $T_m$  values obtained at 0, 600, and 1200 mM NaCl coincided with each other, indicating unaltered conformational stability of apoNCS under high salt conditions.

### 2.2.2. Drug regulation by NCS protein was not affected by salt

The release of NCS-C from holoNCS is the initial key step in the mode of NCS action but the release mechanism has not been fully understood. Early studies suggested that denaturants effectively release NCS-C and stimulate DNA cleavage.<sup>8,23,24</sup> Evidences also show that NCS-C release can be triggered without denaturation.<sup>25,26</sup> By titrating apoNCS with NaCl (0–1000 mM) at pH 7 and 25 °C, we found no significant changes on the resultant CD spectrum of apoNCS (data not shown), suggesting that denaturation was not occurred. However, possibility of NCS-C release triggered by salt without denaturation could not be excluded by this simple titration experiment. We undertook a direct approach by measuring the rate of NCS-C release in salt using excess GSH as a

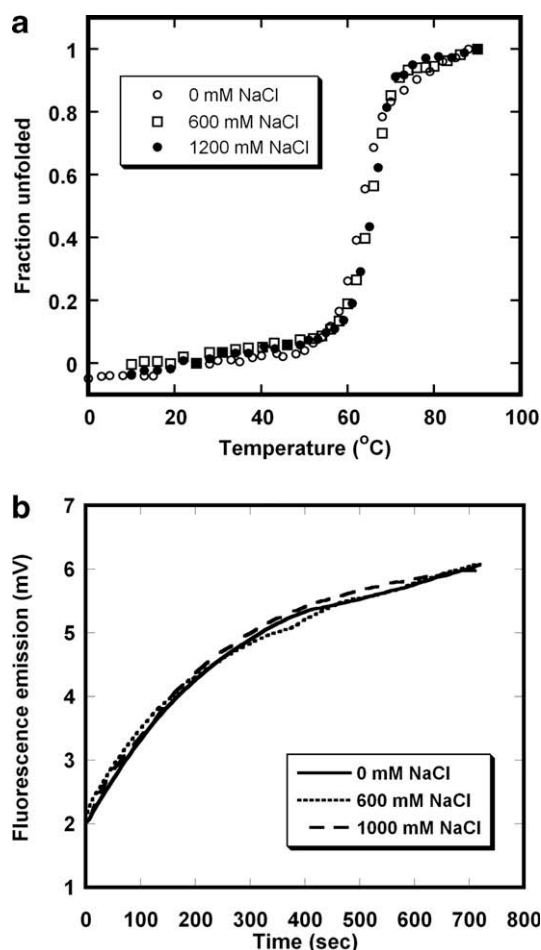


**Figure 2.** Effect of salt on NCS protein stability and chromophore binding ability. (a) Comparison of thermal stability of apoNCS stability in 0 mM (open circle), 600 mM (open square), and 1200 mM NaCl (closed circle). Changes of the secondary structure of apoNCS were monitored by far-UV CD at 224 nm. (b) Comparison of the rate of NCS-C release from holoNCS in 0 mM (solid line), 600 mM (dotted line), and 1000 mM NaCl (broken line). Fluorescence of 5  $\mu$ M holoNCS was measured at 25 °C from the time of adding 5 mM GSH, which converts the released NCS-C into a highly fluorescent GSH–NCS–C adduct.

release indicator, which reacts quickly with unbound NCS-C to form a highly fluorescent adduct.<sup>25</sup> Figure 2b shows largely overlapped release profiles obtained at 0–1000 mM NaCl, demonstrating negligible effect of high salt on the rate of NCS-C release.

### 2.3. NCS-C activation was not inhibited by salt

NCS-C is activated by a thiol to form an active radical intermediate,<sup>5</sup> which abstracts hydrogen to form a stable and inactive thiol–NCS–C adduct (Scheme 1a). To clarify whether salt inhibits thiol-induced activation, we examined formation of GSH–NCS–C adduct<sup>27</sup> at different salt level. The overlaying HPLC profiles illustrated comparable yield of GSH–NCS–C adduct (peak I in Fig. 3) in 0–800 mM NaCl, reflecting trivial effect of salt on the drug activation process. Two minor but salt-dependent products, II and III, were also observed along with I. Because prolonged incubation led to increases of II and III at expenses of I, II and III were likely the degradation products of I.

### 2.4. NCS–C–DNA binding was hampered by salt

Though not effective as apoNCS, DNA protects labile NCS-C from spontaneous degradation in aqueous environment through binding.<sup>10</sup> By following fluorescence changes, kinetic changes of NCS-C degradation from absence to presence of DNA can thus be used to estimate binding affinity of NCS-C and DNA.<sup>10,11</sup> Addition of sodium phosphate buffer was reported to lower the ability of DNA to protect NCS-C.<sup>11</sup> By adding NaCl into NCS-C samples containing a fixed molar ratio of ct-DNA, we observed similar effect. Figure 4a shows evident increases of NCS-C degradation with increasing salt concentrations and demonstrates substantial salt inhibition in DNA-afforded NCS-C protection. Table 1b lists all kinetic results of NCS-C degradation obtained without or with ct-DNA at 0–700 mM NaCl. At 0 mM NaCl, the lifetime ( $\tau$ ) of NCS-C in an aqueous solution (containing 5% methanol at pH 7 and 25 °C) measured without and with ct-DNA (P:D = 100) was 17 and 250 s, respectively, which were reasonably close to those reported (16 and 225 s) measured at pH 7, 22 °C, 0.32% methanol, and P:D = 86.<sup>11</sup>

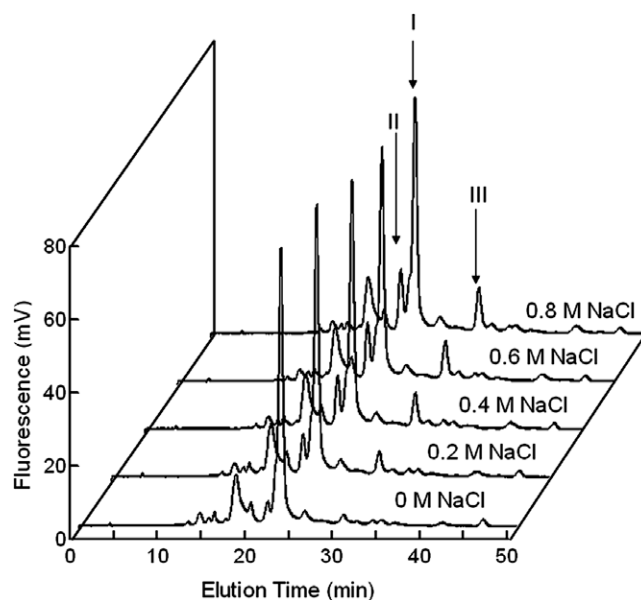


**Figure 3.** Effect of salt on NCS-C activation. HPLC analyses of the GSH-activated NCS-C reaction in 0–800 mM NaCl. The reaction was performed at 0 °C and pH 7.4 in 50% methanol, and the elution profile was recorded by fluorescent emission at 440 nm (excited at 340 nm). Peak I denotes the post-activated GSH–NCS–C adduct and peaks II and III are degraded products of peak I.



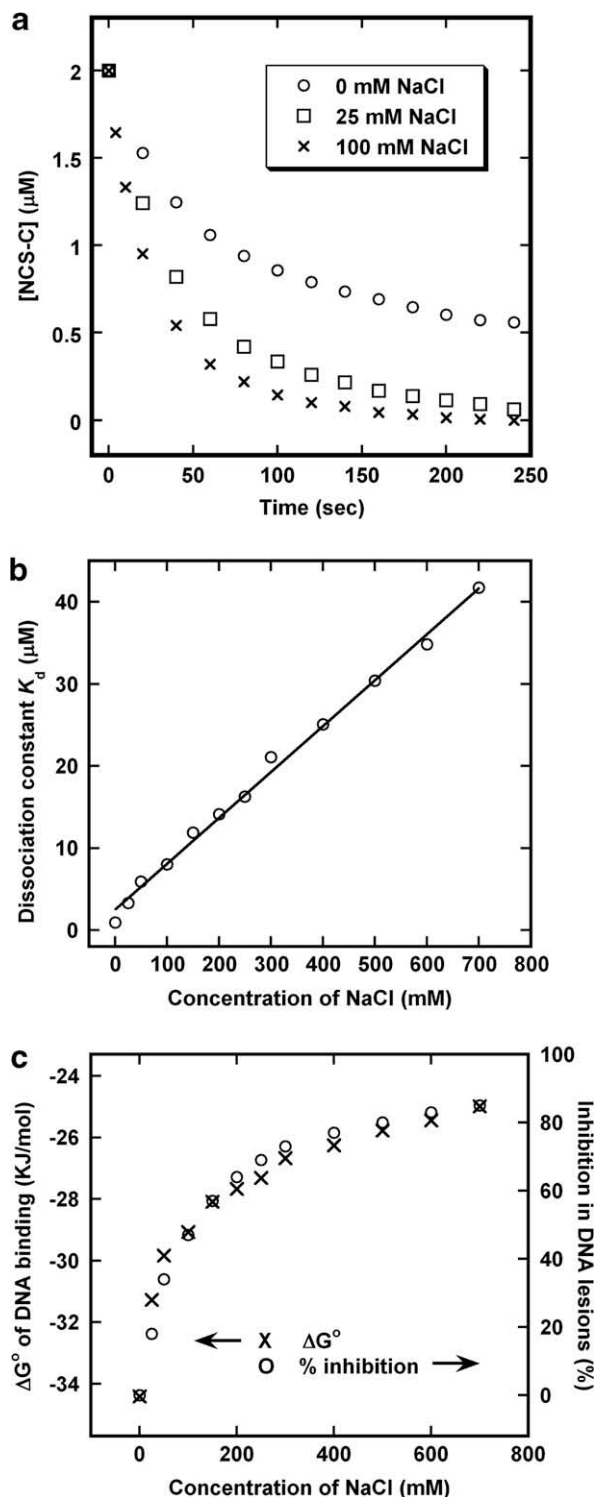


**Figure 4.** Effect of salt on NCS-C–DNA binding. (a) Protection of NCS-C from degradation afforded by DNA in 0 mM (open circle), 25 mM (open square), and 100 mM NaCl (crossed lines). Degradation of NCS-C in the presence of ct-DNA (P:D = 100) at pH 7 and 25 °C was followed by fluorescent emission at 490 nm (excited at 380 nm). (b) Relationship between the concentration of NaCl and the equilibrium dissociation constant of NCS-C–DNA binding complex obtained at pH 7 and 25 °C. (c) Salt-induced changes on  $\Delta G^\circ$  (crossed lines) of DNA binding and mean % of inhibition (open circle) of NCS activity in inducing DNA lesions.

At 150 mM NaCl, the degradation rate of NCS-C in the absence of DNA did not show significant changes (see  $k_0$  in Table 1b). By contrast, the degradation rate increased sharply to more than sixfolds in the presence of DNA (see  $k_{\text{DNA}}$  in Table 1b). Because degradation

rate is proportional to the equilibrated fraction of unbound NCS-C, the equilibrium dissociation constant  $K_d$  can be estimated from  $k_0$  and  $k_{\text{DNA}}$ .<sup>10</sup> The  $K_d$  value was close to 1 μM at 0 mM NaCl and increased with increasing concentration of NaCl (Table 1b). Figure 4b shows a good linear correlation between  $K_d$  and concentration of NaCl (correlation coefficient  $R = 0.9975$  with a slope of increasing  $K_d$  of 5.6 μM per additional 100 mM of NaCl). Apparently, the presence of salt efficiently eliminated the ability of DNA to protect NCS-C by weakening the binding affinity of DNA.

### 3. Discussion

#### 3.1. Salt influence examined in each of the four consecutive steps of NCS action

The mode of NCS action mainly involves four consecutive steps: (step 1) releasing of NCS-C from NCS protein; (step 2) binding of NCS-C to DNA; (step 3) activating of NCS-C by thiol; and (step 4) DNA damaging reactions. We attempted to elucidate the inhibition mechanism on molecular basis by analyzing the salt influence on each step of NCS action. We examined interactions of salt with apoNCS, holoNCS, or NCS-C, and thoroughly analyzed salt influence on the DNA damaging level for each type of lesion.

#### 3.2. No salt effect observed on the releasing, activating, and DNA damaging steps

ApoNCS controls drug activity by protecting and regulating NCS-C.<sup>5</sup> We compared the drug activity of holoNCS and NCS-C in salt solutions and observed no differentials. By CD measurement, we found that neither the backbone structure, nor the stability of the protein was altered by high salt. The kinetic rate of NCS-C release from carrier protein showed no changes in high salt solutions. Collectively, the results excluded participation of NCS protein in salt inhibition mechanism. Furthermore, HPLC analyses on the thiol-induced drug activating reaction (Scheme 1a) suggested negligible effect of salt. For DNA damaging actions, direct strand breaks and abasic site lesions are resulted from hydrogen abstractions followed by oxidative reactions involving oxygen and thiol (Scheme 1b).<sup>5</sup> The lesion level (SS, DS or TS) depends upon thiol structures<sup>3,9</sup> and types of DNA damaging reactions.<sup>5</sup> Surprisingly, the % inhibition by salt was found independent to lesion types and thiol structures (Fig. 1 and Table 1a), suggesting no involvement of salt in the DNA-damaging reactions.

#### 3.3. Salt inhibited binding of NCS-C to DNA

By measuring the degradation rate of NCS-C, the ability of DNA to protect NCS-C was found to decrease sharply with increasing salt concentration. Meanwhile, the observed  $K_d$  of drug–DNA binding complex increased linearly with salt concentration, suggesting that salt was the sole cause to interfere DNA binding. We evaluated the drug–DNA binding affinity by changes of Gibbs' Free Energy ( $\Delta G^\circ$ ) (from  $\Delta G^\circ = -RT \ln(1/K_d)$ ) and compared it with % inhibition at the same salt level. Figure 4c shows hyperbolic dependencies that agreed well between changing trend of % inhibition on drug activity and  $\Delta G^\circ$  for DNA binding, confirming a close correspondence of the salt inhibition with the weakened DNA binding affinity. Direct interference of DNA binding by salt, therefore, was the main and sole cause for the salt inhibition.

#### 3.4. Possible interactions of salt with DNA

Early study shows that the DNA helix unwinds 21° by NCS-C binding and elongates nearly 3.3 Å for each bound NCS-C mole-

**Table 1**

Effect of salt on: (a) NCS-induced DNA lesions; and (b) binding of NCS-C with DNA

Concd of NaCl (mM)	(a) Mean value <sup>a</sup> of % inhibition in NCS-induced DNA lesions obtained at various conditions	(b) Binding of NCS-C with DNA <sup>b</sup>		
		Rate constant of NCS-C degradation w/o DNA, $k_0$ (min <sup>-1</sup> )	Rate constant of NCS-C degradation w DNA, $k_{DNA}$ (min <sup>-1</sup> )	Dissociation constant $K_d$ (μM)
0	0	3.47	0.240	0.929
25	18 ± 3	3.45	0.720	3.30
50	34 ± 3	3.44	1.10	5.91
100	47 ± 3	3.32	1.30	8.05
150	57 ± 4	3.08	1.51	11.9
200	64 ± 4	2.94	1.56	14.1
250	69 ± 4	2.82	1.60	16.3
300	73 ± 5	2.58	1.62	21.1
400	77 ± 5	2.45	1.64	25.1
500	80 ± 5	2.33	1.65	30.4
600	83 ± 5	2.25	1.66	34.8
700	85 ± 5	2.16	1.66	41.7

<sup>a</sup> Mean value of % inhibition with standard deviation were averaged from the data obtained at various conditions including: BME-activated holoNCS-induced DNA direct TS, SS, and DS breaks at 37 °C; BME-activated NCS-C-induced DNA direct TS, SS, and DS breaks at 0 °C; BME-activated holoNCS-induced and putrescine-expressed DNA TS, SS, and DS lesions (summation of direct strand breaks and abasic site lesions) at 37 °C; BME-activated NCS-C-induced and putrescine-expressed DNA TS, SS, and DS lesions at 0 °C; GSH-activated holoNCS-induced DNA direct TS, SS, and DS breaks at 37 °C; GSH-activated NCS-C-induced DNA direct TS, SS, and DS breaks at 0 °C; GSH-activated holoNCS-induced and putrescine-expressed DNA TS, SS, and DS lesions at 37 °C; GSH-activated NCS-C-induced and putrescine-expressed DNA TS, SS, and DS lesions at 0 °C, etc. Under each specified condition the data were averaged from minimum of 3 repeats within 10% SD.

<sup>b</sup> The first-order degradation rate constant of NCS-C (1 μM) in the absence ( $k_0$ ) or presence ( $k_{DNA}$ ) of ct-DNA (molar ratio of nucleotide phosphorus to drug (P:D) = 100) was determined at pH 7 and 25 °C by fluorescence spectroscopy. The methanol content (introduced from NCS-C stock solution), which affects degradation rate of NCS-C, was kept constant for each sample (5% (v/v)).  $K_d$ , the equilibrium dissociation constant of DNA–NCS-C binding complex, was estimated from  $k_0$  and  $k_{DNA}$  (see Section 5). All values were averaged from minimum of 3 repeats within 10% SD.

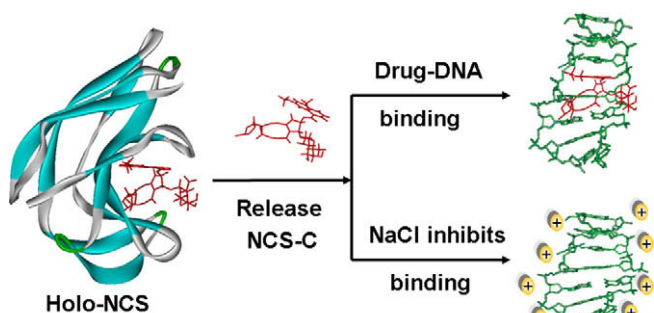


**Figure 5.** Model illustrating that significant effect on the drug activity solely resulted from salt inhibition in enediyne–DNA binding.

cule.<sup>11</sup> Three-dimensional drug–DNA binding structure has been resolved by replacing labile NCS-C with the stable post-activated GSH–NCS-C adduct.<sup>28–30</sup> The model structure reveals a binding mode with intercalation of the naphthoate moiety at minor groove, which unwinds and stretches relative to the helical axis and exhibits buckled base pairs at the intercalation site. The positively charged  $\text{Na}^+$  may substantially stabilize DNA conformation by reducing electrostatic repulsion between intra strand phosphates.<sup>31</sup> The salt interactions thus make DNA helix more rigid against unwinding and elongation caused by drug binding. As illustrated in Figure 5, the presence of NaCl could successfully impose restriction on intercalation of the planar naphthoate moiety of NCS-C between adjacent base pairs of DNA.

#### 4. Conclusion

Although the enediyne antibiotic category belongs to one of the most potent antitumor agents, its application is often limited by high toxicity and also in vivo efficacy. Using the first enediyne NCS as a model, we demonstrated substantial decrease of the drug activity by merely ordinary salt. The salt effect on the NCS activity was very significant with half-efficiency (50% inhibition) occurred at a salt concentration of only about 110 mM, which is far below than the concentration in mammalian blood. While salt caused

up to  $85 \pm 5\%$  inhibition on the drug-induced DNA lesions, interestingly, it did not alter or quench the inherent high activity of the active radical species of NCS. Salt played its important role only in interfering the drug–DNA binding, which critically influenced the drug activity.

## 5. Materials and methods

### 5.1. Materials

HoloNCS in powder form was from Kayaku Co. Ltd, Japan. It was dissolved in water at a concentration of 5 mM and stored in dark at  $-80^\circ\text{C}$ . NCS-C was prepared by repetitive extraction from lyophilized holoNCS stock in 20 mM sodium citrate, pH 4.0/methanol.<sup>3</sup> Integrity of NCS-C was confirmed by high performance liquid chromatography (HPLC) analysis as described.<sup>27</sup> Concentration of NCS-C stock was determined by measuring: (1) peak integration on the HPLC profile at 226 nm; and (2) increased  $A_{340}$  ( $\epsilon$ , 10,800) following titration into excess apoNCS using a UV–vis spectrophotometer. All other reagents used were analytical grade.

### 5.2. NCS–DNA reaction

Native plasmid DNA pBR322 was purified from *Escherichia coli* DH5 $\alpha$  harboring the plasmid DNA using Mini-Prep plasmid isolation kit (Qiagen Inc., Hilden, Germany). The absorbance ratio  $A_{260/280}$  of DNA was 1.8–1.9, indicating that the DNA was sufficiently free of protein. To study the effect of salt on NCS-mediated DNA lesions, NaCl at a wide range of concentration (0–700 mM) was added to the NCS–DNA reaction mixture. Samples contained 5 mM ammonium acetate (pH 4.0), 200 ng supercoiled pBR322, 3 mM EDTA (pH 4.0), 5–20 nM holoNCS or NCS-C, and 5 mM glutathione (GSH) or 10 mM 2-mercaptoethanol (BME) were mixed with salt under acidic condition. Tris–HCl (pH 7.4) was added to a final concentration of 100 mM to initiate the NCS–DNA reaction. The final volume of each sample was 36  $\mu\text{L}$  with methanol content below 10% (v/v) (introduced from methanolic NCS-C stock). Samples were incubated for 30 min in dark at 37 °C for holoNCS- or 0 °C for NCS-C–DNA reaction. Direct strand breaks of DNA were analyzed by following electrophoresis of reaction samples immedi-

ately after incubation. To convert all abasic site DNA lesions to strand breaks and to assess the total DNA lesions, putresine at pH 8.0 was added to a final concentration of 100 mM after incubation. Samples were further incubated for 1 h at room temperature prior to analysis.<sup>3,9</sup>

### 5.3. Electrophoresis and DNA lesion analysis

The NCS-cleaved DNA fragments were analyzed by a 1% agarose gel with ethidium bromide (0.5 µg/ml) in a mini electrophoresis apparatus (Hoefer Scientific instrument, San Francisco, USA). Bands representing the three topological forms were documented in a fluorimager Alpha Imager 2000 (Alpha Innotech Corp., USA). Fractions of supercoiled (form I), relaxed circular (form II), and linear duplex (form III) molecules were determined from integration of the respective bands. Because of the least ethidium bromide staining, form I fluorescence intensity was corrected given its only 70% as compared with form II and III. Number of total strand (TS) breaks ( $N_{TS}$ ) per DNA molecule induced by NCS was calculated from fraction of the remaining form I ( $f_I$ ) following the Poisson distribution:  $N_{TS} = -\ln(f_I/f_{I_0})$ , where  $f_{I_0}$  is the fraction of form I in control.<sup>3,9,32</sup> The number of double-strand breaks ( $N_{DS}$ ) per DNA molecule was calculated from the fraction of form III ( $f_{III}$ ) following the equation:  $\ln(N_{DS}) - N_{DS} = \ln(f_{III}/f_{I_0})$ . The number of single-strand breaks ( $N_{SS}$ ) was calculated from the difference between number of TS and DS:  $N_{SS} = N_{TS} - N_{DS}$ .

### 5.4. Thermal stability measurement

ApoNCS samples at a final concentration of 20 µM were prepared in 20 mM sodium phosphate (pH 7.0) containing 0, 200, 400, 600, 1200, or 1500 mM NaCl. The circular dichroic (CD) signals were recorded on a Jasco J715 spectropolarimeter (Tokyo, Japan) equipped with a Neslab (Portsmouth, NH, USA) model RTE-140 circulating water bath. Thermal-induced unfolding of apoNCS was measured by following changes of far-UV CD signals at 224 nm in a temperature range of 0–100 °C using a water-jacketed quartz cell (0.1 cm path length). The temperature of the water bath was controlled by a microprocessor and temperature sensor. Because equilibrium was reached within 10 min after changing temperatures, equilibrium time was set at 15 min for each increment of temperature (3 °C).<sup>22</sup>

### 5.5. NCS-C release measurement

Salt effect on the release rate of NCS-C from holoNCS was assessed by monitoring fluorescence changes by a SLM-Aminco Bowman series 2 model Luminescence Spectrofluorimeter (SLM Aminco Bowman, Urbana, IL, USA). Samples of holoNCS (5 µM) were prepared in 100 mM of Tris-HCl (pH 7.4) containing 0, 400, 600, 800, or 1000 mM NaCl. Release of NCS-C was followed at 25 °C from the time of addition of 5 mM GSH. A single point acquisition for fluorescence emission at 440 nm in mV (excitation at 340 nm) was collected every 30 s. The shutter was closed in between each measurement to avoid photo degradation of NCS by the excitation light.<sup>26</sup>

### 5.6. HPLC analysis of thiol-activated reaction of NCS-C

Samples of thiol-NCS-C reaction were prepared in a final volume of 100 µl by mixing 10 µM NCS-C, 1 mM ammonium acetate (pH 4), 3 mM EDTA (pH 4), 5 mM GSH, 50% methanol, 0–800 mM NaCl, and 100 mM Tris-HCl (pH 7.4). Each reagent was pre-cooled and Tris-HCl was added last. The samples were incubated at 0 °C for 5 min prior to HPLC analysis. The yield of the post-activated GSH-NCS-C adduct was analyzed by a Waters µ-Bondapak reverse

phase C<sub>18</sub> column using a Waters Millennium HPLC (Milford, MA, USA) equipped with a model 600E solvent delivery system, a 996 photodiode array detector and either a Waters 474 or a Jasco FP-1520 fluorescence detector (Tokyo, Japan) following the previously described method.<sup>27</sup>

### 5.7. NCS-C-DNA binding study

Calf-thymus DNA (ct-DNA) (Sigma, St. Louis, MO, USA) was sonicated (~400 bp) and purified as described.<sup>3,10</sup> Binding affinity of NCS-C to ct-DNA was estimated by NCS-C degradation kinetics in the absence and presence of DNA monitored by a SLM-Aminco Bowman series 2 model Luminescence Spectrofluorimeter (SLM Aminco Bowman, Urbana, IL, USA). NCS-C stocks in a concentration of 20–100 µM were prepared by dilution of the acidic methanol-extracted NCS-C with methanolic 5 mM ammonium acetate (pH 4). Samples in a final volume of 150 µl were prepared by mixing 0–700 mM NaCl, 20 mM phosphate buffer (pH 7), and 1–5 µM NCS-C in the absence or presence of 100–500 µM ct-DNA (concentration in nucleotide phosphate). The molar ratio of DNA nucleotide phosphorus to drug (P:D) and methanol content (introduced from NCS-C stock) were kept constant as 100 and 5% (v/v), respectively, for all samples. The NCS-C was added last, immediately prior to fluorescence measurement. By excitation at 380 nm, the emission at 490 nm was recorded in a time scan mode until it reached a plateau (indicating the spontaneous degradation reaction of NCS-C was complete). The remaining concentration of NCS-C ( $[NCS-C]$ ) was determined by:  $[NCS-C] = [NCS-C]_0 - \{F_t/(F_\infty - F_0)\} \times [NCS-C]_0$ , where  $[NCS-C]_0$  is the initial concentration;  $F_t$  is the measured fluorescent emission at time  $t$ ;  $F_0$  is the initial reading; and  $F_\infty$  is the plateau reading. The first-order degradation rate constant of NCS-C in the absence ( $k_0$ ) or presence ( $k_{DNA}$ ) of ct-DNA was determined by the slope of linear plot of logarithmic  $[NCS-C]$  versus time. The apparent equilibrium dissociation constant ( $K_d$ ) of the NCS-C-DNA binding complex was determined by the derived equation:<sup>11</sup>  $K_d = [DNA]_f^* / ((k_0/k_{DNA}) - 1)$ , where  $[DNA]_f^*$  corresponds to the concentration of free binding site on DNA. Since there is 0.125 high affinity NCS-C binding sites per nucleotide,  $[DNA]_f^*$  is equivalent to 0.125 times of the total DNA nucleotide concentration.<sup>11</sup>

### Acknowledgments

We thank Ms. Chiy-Mey Huang for performing HPLC analysis and Dr. P. Vijaya Palani for preparing the preliminary draft. We also thank the Kayaku Co., Ltd, for the supply of NCS powder. This work was supported by a Laboratory Grant (NHRI-EX90-8807BL) from National Health Research Institutes, and Individual Grants (95-2311-B-005-012-MY3, 95-2113-M-005-007-MY3) from National Science Council, Taiwan, Republic of China. This work was also supported in part by the Ministry of Education, Taiwan, Republic of China, under the ATU plan to National Chung Hsing University.

### References and notes

- Ishida, N.; Miyazaki, K.; Kumagai, K.; Rikimaru, M. *J. Antibiot. (Tokyo) Ser. A* **1965**, 18, 68.
- Edo, K.; Mizugaki, M.; Koide, Y.; Seto, H.; Furihata, K.; Otake, N.; Ishida, N. *Tetrahedron Lett.* **1985**, 26, 331.
- Kuo, H.-M.; Lee Chao, P.-D.; Chin, D.-H. *Biochemistry* **2002**, 41, 897.
- Stubbs, M.; McSheehy, P. M.; Griffiths, J. R.; Bashford, C. L. *Mol. Med. Today* **2000**, 6, 15.
- Goldberg, I. H. *Acc. Chem. Res.* **1991**, 24, 191.
- Albers-Schonberg, G.; Dewey, R. S.; Hensens, O. D.; Liesch, J. M.; Napier, M. A.; Goldberg, I. H. *Biochem. Biophys. Res. Commun.* **1980**, 95, 1351.
- Kappen, L. S.; Goldberg, I. H. *Biochemistry* **1980**, 19, 4786.
- Jung, G.; Kohnlein, W. *Biochem. Biophys. Res. Commun.* **1981**, 98, 176.
- Dedon, P. C.; Goldberg, I. H. *Biochemistry* **1992**, 31, 1909.
- Povirk, L. F.; Goldberg, I. H. *Biochemistry* **1980**, 19, 4773.

11. Povirk, L. F.; Dattagupta, N.; Warf, B. C.; Goldberg, I. H. *Biochemistry* **1981**, *20*, 4007.
12. Myers, A. G. *Tetrahedron Lett.* **1987**, *28*, 4493.
13. Chin, D.-H.; Zeng, C. H.; Costello, C. E.; Goldberg, I. H. *Biochemistry* **1988**, *27*, 8106.
14. Powell, S. N.; Abraham, E. H. *Cytotechnology* **1993**, *12*, 325.
15. Kappen, L. S.; Goldberg, I. H.; Liesch, J. M. *Proc. Natl. Acad. Sci. U.S.A.* **1982**, *79*, 744.
16. Kappen, L. S.; Goldberg, I. H. *Biochemistry* **1983**, *22*, 4872.
17. Chin, D.-H.; Kappen, L. S.; Goldberg, I. H. *Proc. Natl. Acad. Sci. U.S.A.* **1987**, *84*, 7070.
18. Kappen, L. S.; Goldberg, I. H.; Frank, B. L.; Worth, L., Jr.; Christner, D. F.; Kozarich, J. W.; Stubbe, J. *Biochemistry* **1991**, *30*, 2034.
19. Povirk, L. F.; Houlgrave, C. W. *Biochemistry* **1988**, *27*, 3850.
20. Sudhahar, C. G.; Chin, D.-H. *Bioorg. Med. Chem.* **2006**, *14*, 3543.
21. Kandaswamy, J.; Hariharan, P.; Kumar, T. K.; Yu, C.; Lu, T. J.; Chin, D.-H. *Anal. Biochem.* **2008**, *381*, 18.
22. Jayachithra, K.; Kumar, T. K. S.; Lu, T.-J.; Yu, C.; Chin, D.-H. *Biophys. J.* **2005**, *88*, 4252.
23. Kappen, L. S.; Goldberg, I. H. *Nucleic Acids Res.* **1978**, *5*, 2959.
24. Kappen, L. S.; Goldberg, I. H. *Biochemistry* **1979**, *18*, 5647.
25. Sudhahar, G. C.; Balamurugan, K.; Chin, D.-H. *J. Biol. Chem.* **2000**, *275*, 39900.
26. Hariharan, P.; Liang, W.; Chou, S.-H.; Chin, D.-H. *J. Biol. Chem.* **2006**, *281*, 16025.
27. Chin, D.-H.; Tseng, M.-C.; Chuang, T.-C.; Hong, M.-C. *Biochim. Biophys. Acta* **1997**, *1336*, 43.
28. Gao, X.; Stassinopoulos, A.; Gu, J.; Goldberg, I. H. *Bioorg. Med. Chem.* **1995**, *3*, 795.
29. Gao, X.; Stassinopoulos, A.; Rice, J. S.; Goldberg, I. H. *Biochemistry* **1995**, *34*, 40.
30. Gao, X.; Stassinopoulos, A.; Ji, J.; Kwon, Y.; Bare, S.; Goldberg, I. H. *Biochemistry* **2002**, *41*, 5131.
31. Hagerman, P. J. *Annu. Rev. Biophys. Biophys. Chem.* **1988**, *17*, 265.
32. Povirk, L. F.; Wubker, W.; Kohnlein, W.; Hutchinson, F. *Nucleic Acids Res.* **1977**, *4*, 3573.